

NASA/TM—2015–218202



# **Proof-of-Concept Experiments on a Gallium-Based Ignitron for Pulsed Power Applications**

*H.K. Ali, V.S. Hanson, K.A. Polzin, and J.B. Pearson  
Marshall Space Flight Center, Huntsville, Alabama*

---

*February 2015*

## The NASA STI Program...in Profile

Since its founding, NASA has been dedicated to the advancement of aeronautics and space science. The NASA Scientific and Technical Information (STI) Program Office plays a key part in helping NASA maintain this important role.

The NASA STI Program Office is operated by Langley Research Center, the lead center for NASA's scientific and technical information. The NASA STI Program Office provides access to the NASA STI Database, the largest collection of aeronautical and space science STI in the world. The Program Office is also NASA's institutional mechanism for disseminating the results of its research and development activities. These results are published by NASA in the NASA STI Report Series, which includes the following report types:

- **TECHNICAL PUBLICATION.** Reports of completed research or a major significant phase of research that present the results of NASA programs and include extensive data or theoretical analysis. Includes compilations of significant scientific and technical data and information deemed to be of continuing reference value. NASA's counterpart of peer-reviewed formal professional papers but has less stringent limitations on manuscript length and extent of graphic presentations.
- **TECHNICAL MEMORANDUM.** Scientific and technical findings that are preliminary or of specialized interest, e.g., quick release reports, working papers, and bibliographies that contain minimal annotation. Does not contain extensive analysis.
- **CONTRACTOR REPORT.** Scientific and technical findings by NASA-sponsored contractors and grantees.
- **CONFERENCE PUBLICATION.** Collected papers from scientific and technical conferences, symposia, seminars, or other meetings sponsored or cosponsored by NASA.
- **SPECIAL PUBLICATION.** Scientific, technical, or historical information from NASA programs, projects, and mission, often concerned with subjects having substantial public interest.
- **TECHNICAL TRANSLATION.** English-language translations of foreign scientific and technical material pertinent to NASA's mission.

Specialized services that complement the STI Program Office's diverse offerings include creating custom thesauri, building customized databases, organizing and publishing research results...even providing videos.

For more information about the NASA STI Program Office, see the following:

- Access the NASA STI program home page at <<http://www.sti.nasa.gov>>
- E-mail your question via the Internet to <[help@sti.nasa.gov](mailto:help@sti.nasa.gov)>
- Phone the NASA STI Help Desk at 757-864-9658
- Write to:  
NASA STI Information Desk  
Mail Stop 148  
NASA Langley Research Center  
Hampton, VA 23681-2199, USA

NASA/TM—2015–218202



# **Proof-of-Concept Experiments on a Gallium-Based Ignitron for Pulsed Power Applications**

*H.K. Ali, V.S. Hanson, K.A. Polzin, and J.B. Pearson  
Marshall Space Flight Center, Huntsville, Alabama*

National Aeronautics and  
Space Administration

Marshall Space Flight Center • Huntsville, Alabama 35812

---

***February 2015***

## **Acknowledgments**

We appreciate continuing management support of Jim Martin, and appreciate the support of Adam Martin, Richard Eskridge, and Tommy Reid in the setup and execution of the gallium ignitron testing. Hisham Ali was supported through a NASA Space Technology Research Fellowship, grant number NNX13AL82H. Valerie Hanson was supported through the Summer 2010 Marshall Space Flight Center NASA Academy program.

## **TRADEMARKS**

Trade names and trademarks are used in this report for identification only. This usage does not constitute an official endorsement, either expressed or implied, by the National Aeronautics and Space Administration.

Available from:

NASA STI Information Desk  
Mail Stop 148  
NASA Langley Research Center  
Hampton, VA 23681-2199, USA  
757-864-9658

This report is also available in electronic form at  
<<http://www.sti.nasa.gov>>

## TABLE OF CONTENTS

1. INTRODUCTION .....	1
2. BACKGROUND .....	3
3. PROPERTIES OF GALLIUM AND MERCURY .....	8
4. EXPERIMENTAL APPARATUS .....	10
5. EXPERIMENTAL DATA .....	13
6. DISCUSSION .....	16
7. FUTURE DESIGN IMPROVEMENTS .....	17
8. CONCLUSIONS .....	18
9. REFERENCES .....	19



## LIST OF FIGURES

1.	Basic ignitron schematic .....	4
2.	Schematic of an ignitron incorporating design elements to mitigate arc migration .....	6
3.	Gallium and mercury vapor pressure as a function of temperature .....	9
4.	Design of the experimental apparatus .....	11
5.	Schematic showing the setup of the ignitron charge circuit, trigger pulse paths, and data systems used .....	12
6.	Waveforms for (a) voltage and (b) current 2-kV gallium ignitron discharge with markers indicating the times for the images in figure 7 .....	14
7.	Selected images of a 2-kV gallium ignitron discharge obtained at a frame rate of 500 kHz and a gate time of 250 ns (false color of grayscale images). The subfigures correspond to the letters given on the waveforms in figure 6 .....	14
8.	Waveforms for (a) voltage and (b) current for a 3-kV gallium ignitron discharge with markers indicating the times for the images in figure 9 .....	15
9.	Selected images of a 3-kV gallium ignitron discharge obtained at a frame rate of 500 kHz and a gate time of 250 ns (false color of grayscale images). The subfigures correspond to the letters given on the waveforms in figure 8 .....	15

## LIST OF TABLES

1.	Physical properties of gallium and mercury .....	8
2.	Ignition delay and current rise time for 2- and 3-kV discharges .....	13





## NOMENCLATURE

$d$	ignitron diameter
$f$	ignitron firing frequency
$p$	gallium vapor pressure
$t$	time



## TECHNICAL MEMORANDUM

### PROOF-OF-CONCEPT EXPERIMENTS ON A GALLIUM-BASED IGNITRON FOR PULSED POWER APPLICATIONS

#### 1. INTRODUCTION

Ignitrons are electrical switching devices that operate at switching times that are on the order of microseconds, can conduct high currents of thousands of amps, and are capable of holding off tens of thousands of volts between pulses. They consist of a liquid metal pool within an evacuated tube that serves both the cathode and the source of atoms and electrons for an arc discharge. Facing the liquid metal pool is an anode suspended above the cathode, with a smaller ignitor electrode tip located just above the surface of the cathode. The ignitron can be charged to significant voltages, with a potential difference of thousands of volts between anode and cathode. When an ignition pulse is delivered from the ignitor electrode to the cathode, a small amount of the liquid metal is vaporized and subsequently ionized, with the high voltage between the anode and cathode causing the gas to bridge the gap between the two electrodes. The electrons and ions move rapidly towards the anode and cathode, respectively, with the ions liberating still more atoms from the liquid metal cathode surface as a high-current plasma arc discharge is rapidly established. This arc continues in a self-sustaining fashion until the potential difference between the anode and cathode drops below some critical value.

Ignitrons have been used in a variety of pulsed power applications, including the railroad industry, industrial chemical processing, and high-power arc welding.<sup>1</sup> In addition, they might prove useful in terrestrial power grid applications, serving as high-current fault switches, quickly shunting dangerous high-current or high-voltage spikes safely to ground. The motivation for this work stemmed from the fact that high-power, high-reliability, pulsed power devices like the ignitron have been used for ground testing in-space pulsed electric thruster technologies, and the continued use of ignitrons could prove advantageous to the future development and testing of such thrusters.<sup>2</sup> Previous ignitron designs have used mercury as the liquid metal cathode, owing to its presence as a liquid at room temperatures and a vapor pressure of 10 Pa (75 mtorr) at room temperature. While these are favorable properties, there are obvious environmental and personal safety concerns with the storage, handling, and use of mercury and its compounds.

The purpose of the present work was to fabricate and test an ignitron that used as its cathode an alternate liquid metal that was safe to handle and store. To that end, an ignitron test article that used liquid gallium as the cathode material was developed and tested.<sup>3</sup> Gallium is a metal that has a melting temperature of 29.76 °C, which is slightly above room temperature, and a boiling point of over 2,300 °C at atmospheric pressure. This property makes gallium the element with the

largest relative difference between melting and boiling points. Gallium has a limited role in biology, and when ingested, it will be subsequently processed by the body and expelled rather than accumulating to toxic levels.

The next section of this Technical Memorandum (TM) provides background information on the development of mercury-based ignitrons, which serves as the starting point for the development of the gallium-based variant. Afterwards, the experimental hardware and setup used in proof-of-concept testing of a basic gallium ignitron are presented. Experimental data, consisting of discharge voltage and current waveforms as well as high-speed imaging of the gallium arc discharge in the gallium ignitron test article, are presented to demonstrate the efficacy of the concept. Discussion of the data and suggestions on improvements for future iterations of the design are presented in the final two sections of this TM.

## 2. BACKGROUND

The ignitron is a type of metal vapor switch. The first metal vapor switches were introduced in the early 20th century for high-power rectification. Metal vapor switches are distinguished by the composition of the metal vapor they contain, the operation of their electron source, and the overall controllability of the device. The first and most common metal used for metal vapor switches was mercury, owing to its relatively high vapor pressure and the fact that it exists as a liquid at room temperature. In addition, mercury does not easily 'plate' or deposit in a film on surfaces, instead tending to exhibit adherence to itself.

Many types of mercury vapor switches have been previously applied, from very large steel tank rectifiers for the electrical utility industry to smaller glass bulb rectifiers.<sup>1</sup> The ignitron, derived from the former type of switch, was first introduced during the 1930s. Its major innovation was to take advantage of improved metal-to-glass vacuum seals, reducing the size to a relatively small package and using a water-cooled metal jacket while including a controllable ignition mechanism. In addition, the thermionic life-limiting cathode used in stainless steel rectifiers was replaced with a self-renewing pool of liquid mercury. The result was a relatively small device for controlled high-power switching that did not have the cooling issues associated with glass bulb discharge tubes or the size issues associated with the large steel tank rectifiers.<sup>1</sup>

Historically, the ignitron has been used for rectification and phase control in electric arc welders and diesel-electric locomotives, and for control of high-power commercial electric grids.<sup>1</sup> Other uses have included low- and medium-frequency pulsed power applications such as magnetic confinement fusion research<sup>3</sup> and electromagnetic metal forming.<sup>1</sup> Advances in solid-state technologies have allowed replacement of the ignitron for the majority of these applications. However, the ignitron still finds itself uniquely positioned for research and development in pulsed high-power applications, owing to the ability to operate at high voltages (thousands of volts) and high currents (>10 kA) that are still far in excess of what can be provided by solid-state switches.<sup>1</sup>

The basic ignitron design, illustrated schematically in figure 1, consists of an anode at the top, a liquid metal cathode at the bottom, and an ignitor tip located just above the cathode surface. These components are situated within an evacuated glass tube that is bonded to a hollow, metallic, water-cooled jacket. The anode at the top of the ignitron is usually quite large to spread the overall current attachment location.

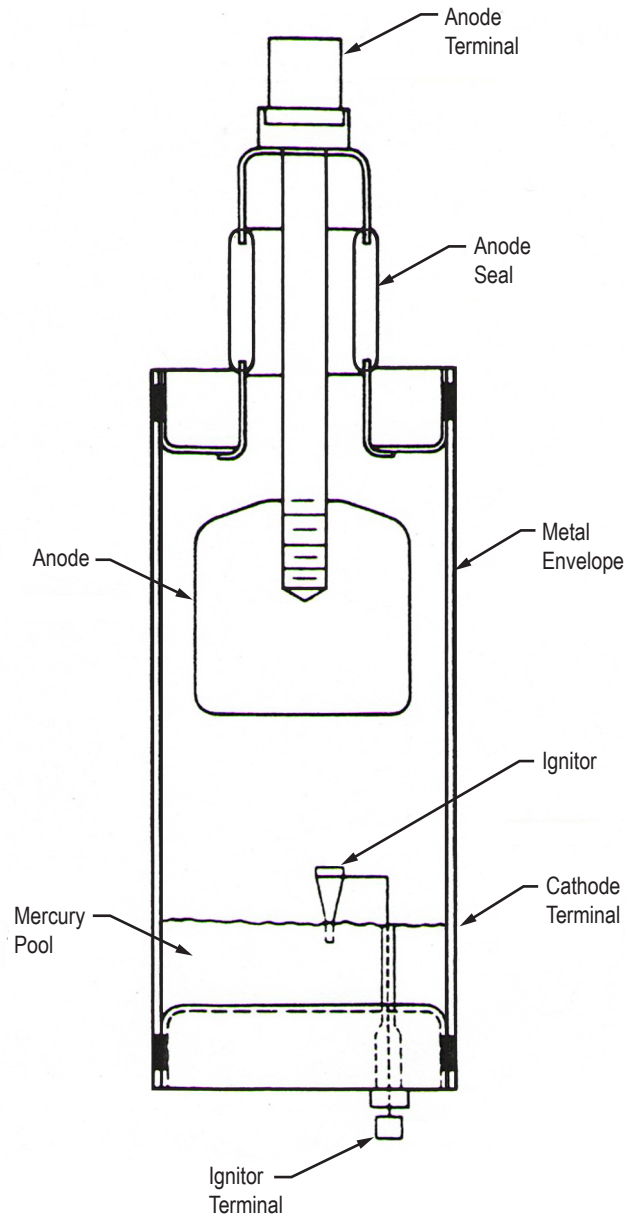


Figure 1. Basic ignitron schematic.

The ignitron is typically connected to a high-voltage source, such as a charged capacitor bank. Ignitron operation begins by first raising the anode to a high voltage. Provided that the maximum voltage hold-off capability has not been exceeded, no conduction will occur between anode and cathode. A discharge in the ignitron is initiated by driving a short ignition pulse between the ignitor and the cathode. The energy from the ignition pulse is concentrated through the ignitor tip into a small area on the liquid cathode surface, forming a hot spot and ejecting metal vapor, metal ions, and free electrons. Cathode spots quickly increase in number and spread from the initial location, resulting in the ejection of additional metal vapor, metal ions, and free electrons.

The free electrons are rapidly accelerated towards the anode, owing to the high electric field present within the ignitron. Initially, the low vapor pressure in the ignitron, which is primarily sourced from the liquid metal cathode, is such that the mean free path for electron-neutral collisions is long enough for the electrons to attain energies greater than the first ionization potential of any encountered gas-phase metal atoms. Collisions with the gaseous metal atoms result in the production of more free electrons through ionizing collisions, with the resultant electrons subsequently accelerated until they collide with additional neutral vapor atoms to produce more electrons in an avalanche breakdown, resulting in a Townsend discharge. Intense heating of the cathode by ions bombarding the surface results in the vaporization of more metal from the cathode and the production of secondary electrons, with the discharge rapidly transitioning from a glow discharge to a low-voltage, high-current arc discharge where thermionic emission occurs. For present mercury vapor ignitrons, this entire process occurs in  $<1 \mu\text{s}$  and represents the characteristic device switching time.<sup>1</sup>

During the discharge, there is a large amount of charge transferred as the voltage between the cathode and anode reduces from its initial level to a much lower  $\approx 10\text{--}100 \text{ V}$ . The ignitor has no control after discharge initiation, and the plasma will only extinguish once the voltage between the cathode and anode falls below a critical arc-sustaining level. In addition to the requirement to reach low voltage for turn-off, there must also be sufficient time for plasma recombination processes to occur, removing the free charge from the ignitron and ‘resetting’ the device for the next switching cycle. The low gas density of the metal vapor minimizes the effectiveness of ion-electron collisions in the plasma recombination process. Instead, recombination is primarily a diffusion-driven process, with the recombination timescale controlled by the number of neutralizing collisions with the side-walls of the device. The resulting characteristic recombination timescale defines the maximum pulse frequency at which an ignitron can be operated. This frequency  $f$  is found to scale roughly as

$$f \sim \frac{1}{pd^2} \quad (1)$$

where  $p$  is the vapor pressure of the liquid metal, and  $d$  is the diameter of the ignitron sidewall.<sup>1</sup>

The failure modes of ignitrons require some consideration. One particularly destructive failure mode involves the tendency of the arc to migrate and attach to the ignitron walls during longer discharges lasting  $>1 \text{ ms}$ . Eventually, this behavior leads to a breaching of the sidewalls, destroying the ignitron. High-current arc discharges are known to produce their own magnetic fields, and these fields can drive so-called ‘sausage’ and ‘kink’ instabilities that will cause the arc to migrate.<sup>4</sup> There are three methods that have been employed to control arc migration in ignitrons.<sup>1</sup>

A schematic of an ignitron that incorporates features to mitigate arc migration is shown in figure 2. The first way in which arc migration is typically mitigated is to ensure that all external conductors are symmetrically arranged. Further mitigation is provided by a mercury splash baffle arc retaining ring, typically comprised of molybdenum and held in place above the cathode pool. When the arc begins migrating to a wall, an enhanced electric field at the surface of the retaining ring stabilizes the arc and keeps it from migrating further in the radial direction. The final technique to mitigate arc migration is to continually energize the ignitor. This provides a continuous supply

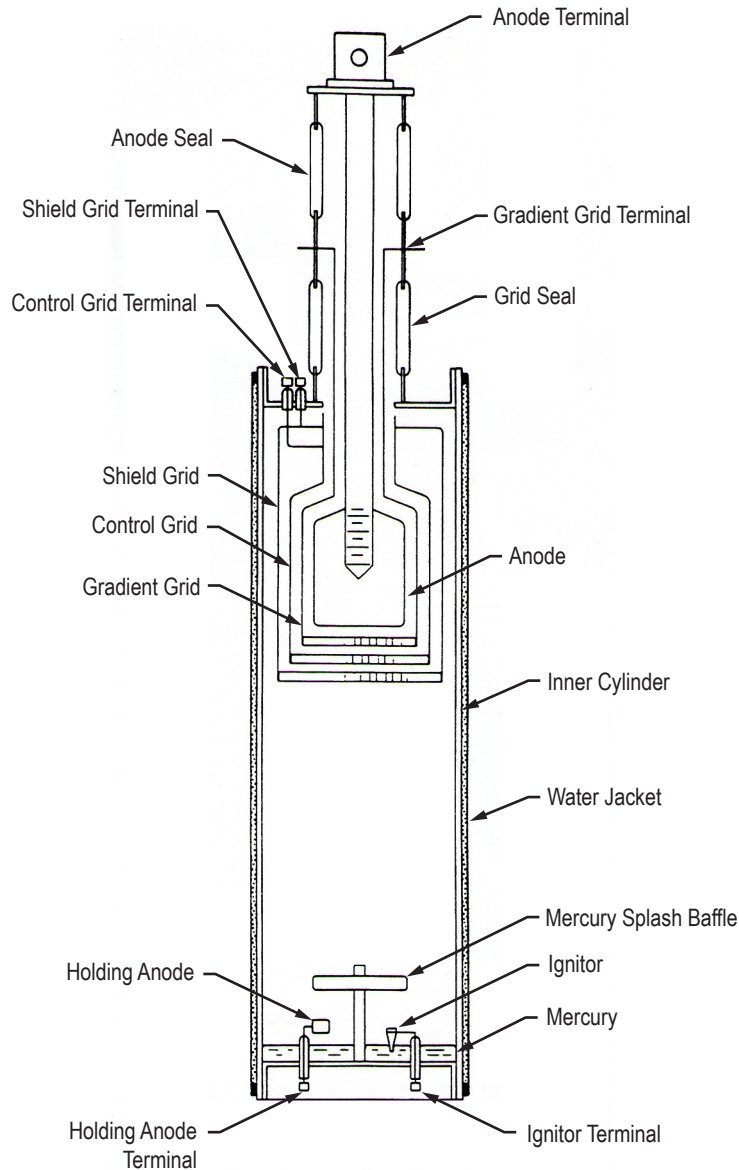


Figure 2. Schematic of an ignitron incorporating design elements to mitigate arc migration.<sup>1</sup>

of metal vapor, metal ions, and free electrons at the cathode surface, ensuring that the arc will stay connected to the cathode surface at that location. The challenge in implementing this technique comes primarily from the complexity of the triggering circuit required to energize the ignitor for periods of 1 ms or greater.

Other ignitron failure modes include condensation of the metal vapor on the anode or insulating tube between the anode and cathode, wetting of the ignitor by the liquid metal cathode, and anode erosion. Condensation of metal vapor on the anode or on the insulator between the electrodes is problematic as it severely limits the voltage hold-off potential of the switch. Typically, this is mitigated through simultaneous heating of the anode and cooling of the cathode to encourage condensation of the metal vapor at the cathode pool. Ignitor wetting and anode erosion are



typically lifetime-limiting issues for ignitrons. The ignitor is designed such that it will not wet under exposure to the pure liquid metal, but as anode erosion occurs over multiple discharges, the erosion products start to appear as impurities in the liquid metal pool, changing the properties from that of the pure liquid metal. Eventually, it becomes possible to form a liquid metal bridge between the ignitor and cathode pool, short-circuiting the ignitor pulse discharge. Anode erosion is avoided to some degree by employing large graphite anodes, which both mitigate anode temperature rise rates due to their size and have low sputter and erosion yields relative to other material options like copper, aluminum, or stainless steel.<sup>1</sup>

### 3. PROPERTIES OF GALLIUM AND MERCURY

In this TM, the writers sought to conduct proof-of-concept experiments on an ignitron where liquid gallium was substituted for mercury. A comparison of the physical properties of gallium and mercury are given in table 1. The standard choice of metal for the liquid cathode in an ignitron has been mercury, owing to its existence as a liquid under normal operating conditions and its relatively modest vapor pressure (see fig. 3). Mercury also does not readily wet insulating surfaces, reducing the likelihood of the formation of a short-circuiting mercury connection between the anode and the cathode. However, the extensive environmental and safety considerations involved with the use and disposal of mercury warrant consideration of other types of liquid metal. Gallium is another metal which is liquid near room temperature but has a much lower vapor pressure and a much higher boiling point than mercury (see table 1 and fig. 3). In addition, gallium has a low toxicity compared to mercury, making it possible to open, clean, and repair a gallium-based ignitron, where a mercury ignitron would have to be discarded.

Table 1. Physical properties of gallium and mercury.

Property	Gallium	Mercury
Mass (amu)	69.723	200.592
Atomic radius (pm)	135	151
Freezing temperature (K)	302.91	234.32
Boiling temperature at 1 atm (K)	2,673	629.88
Heat of fusion (kJ/mol)	5.59	2.29
Molar heat capacity (J/mol)	25.86	27.98
Heat of vaporization (kJ/mol)	254	59.11
First ionization energy (eV)	5.993	10.4427
Vapor pressure at 40 °C (torr)	$1.543 \times 10^{-32}$	$5.005 \times 10^{-2}$

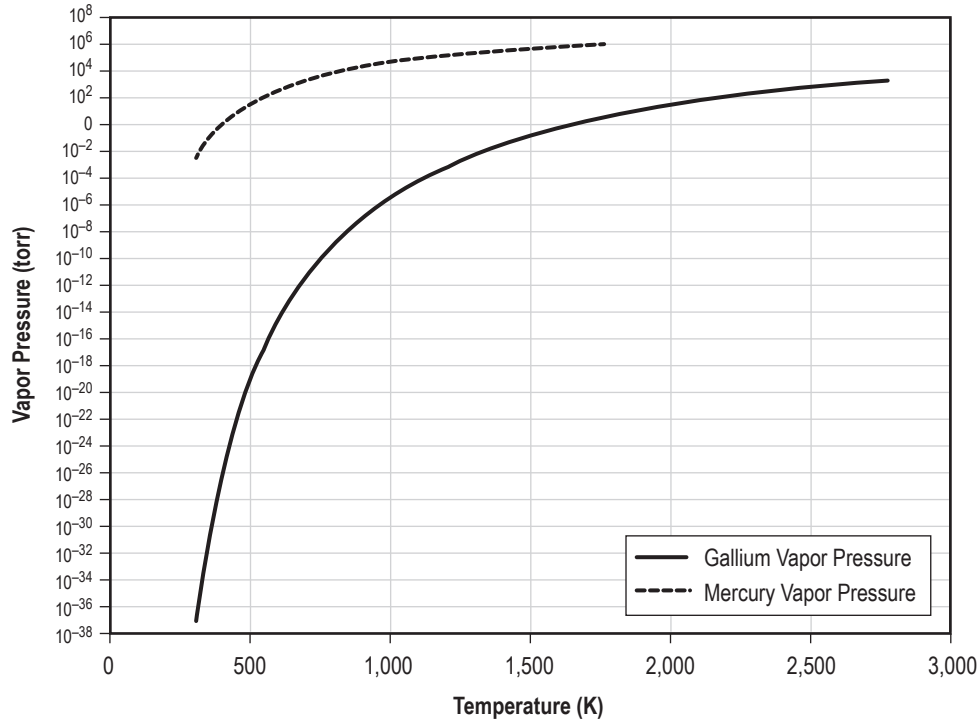


Figure 3. Gallium and mercury vapor pressure as a function of temperature.<sup>5,6</sup>

As can be seen in table 1, gallium has a much higher heat of vaporization and much lower first ionization energy compared to mercury. In light of this comparison, it is expected that gallium will be significantly harder to vaporize, but should be easier to ionize once a gallium vapor is created. For instance, vaporizing 1 mole of gallium initially at 303 K requires 315,370 kJ, while vaporizing 1 mole of mercury requires only 68,397 kJ. However, to vaporize and ionize 1 mole of mercury requires at least 1,075,497 kJ, while doing the same for gallium requires 894,170 kJ. It can thus be hypothesized that if the metal vapor produced during the ignition process is not significantly ionized (weakly ionized limit), then a gallium-based ignitron will require about four times as much energy during the ignition pulse to form a metal vapor. While it requires more energy per mole to vaporize gallium initially, once the main discharge begins the lower combined vaporization and ionization energy of gallium implies that current conduction in a gallium-based ignitron should occur to a lower voltage level as compared to one that is mercury-based.

The vapor pressure of mercury is much higher than that of gallium, with a difference of up to 30 orders of magnitude at lower temperatures. Thus, the equilibrium gas density in a gallium ignitron should be much lower than a mercury ignitron, with the former having a much greater hold-off voltage.

#### 4. EXPERIMENTAL APPARATUS

An illustration of the gallium ignitron used in the present effort is provided in figure 4. A Pyrex tube was employed as the ignitron body because it permits the direct use of optical diagnostics. The tubing used has an outer diameter of 6.35 cm (2.5 in), a 4.8-mm wall thickness, and a length of 30.5 cm (12 in). In addition to permitting optical imaging of the plasma discharge, the glass tube allows for the visual monitoring of oxidization and potential plating. Power was fed to the anode through a Cajon® Ultra-Torr fitting. This fitting uses an o-ring seal on a rod connected to the anode to permit electrode translation without the need to break a seal. The end caps of the test article were fabricated from polyethylene. The bottom end cap consists of a single polyethylene disk with a diameter of 15.25 cm (6 in) and a thickness of 2.5 cm (1 in). Embedded in the bottom end cap is a Watlow® cartridge heater, which can be energized to heat the end cap and maintain the gallium in a liquid state. The top end cap consists of two 12.7-cm- (5-in-) diameter polyethylene disks sandwiched together, with the lower piece having a thickness of 1.25-cm (0.5-in) and the upper piece being 2.5 cm (1 in) thick. Both the bottom end cap and the lower part of the top end cap have a lip machined to permit seating and sealing with the glass tube. The bottom end cap is sealed directly to the glass tube and has holes drilled in it to pass through power feeds to the electrodes. The top part of the top end cap is removable, permitting access to the chamber interior, making it easier to clean the inside and to change anodes if needed. The two pieces are connected using six bolts, with an o-ring vacuum seal between them.

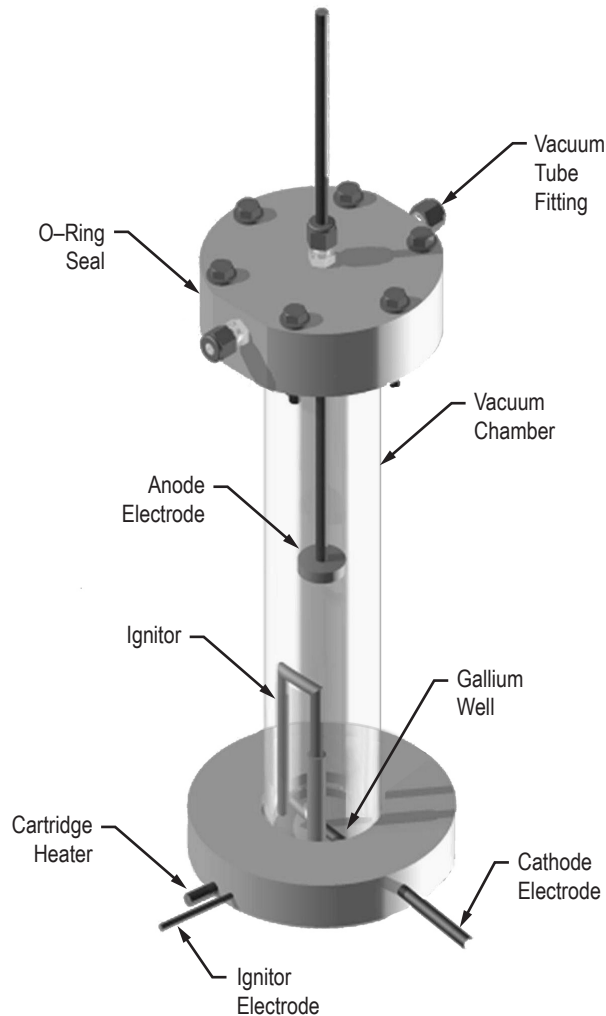


Figure 4. Design of the experimental apparatus.

There are three electrodes: (1) The anode, (2) the cathode, and (3) the ignitor. In prior mercury-based ignitrons, these electrodes have been composed of graphite, molybdenum, titanium, or stainless steel.<sup>7</sup> In this TM, stainless steel was chosen for all three electrodes since it was readily available and is known to be compatible with gallium. The anode is a 2.5-cm- (1-in-) diameter, 6.4-mm- (0.25-in-) thick stainless steel disk welded to a 33-cm- (13-in-) long, 6.4-mm- (0.25-in-) diameter stainless steel rod that passes through the Ultra-Torr fitting. This component can be replaced to permit the testing of different anode materials or geometries. The cathode consists of a liquid gallium pool with a submerged 6.4-mm (0.25-in) stainless steel rod that provides the means of electrical connection between the liquid metal and the rest of the circuit. The ignitor consists of three 6.4-mm- (0.25-in-) diameter stainless steel rod pieces welded together so that the electrode penetrates the vacuum vessel from the bottom before turning back so the tip is just above the liquid gallium surface. The tip is pointed, reducing the surface area in contact with the plasma to enhance the electric field at that location and increase local ohmic heating. Alumina tubing is used to insulate the base of the ignitor from the pool of liquid gallium. The main source of ignitron failure

arises from ignitor breakage or wetting, resulting in very low resistance between the ignitor and cathode pool, greatly reducing the local ohmic heating by short-circuiting the ignitor and cathode.

While the test apparatus was designed to be sealed and evacuated, to minimize the testing time and ensure there would be no vacuum-leak issues, the entire unit was placed inside of a vacuum chamber, with the interior of the Pyrex tube left unsealed. During testing, the apparatus was at the pressure of the vacuum chamber, which was roughly  $10^{-5}$  torr. At large anode-cathode separation distances, there were issues in consistently pulsing the ignitron because the electric field developed between the electrodes at a few kilovolts was insufficient to yield a cascade breakdown. As a consequence, testing was conducted with a small anode-to-cathode distance, but this also brought the anode much closer to the ignitor, which like the cathode, is also at a low potential when not pulsing. As a consequence, additional insulation had to be added to the ignitor to prevent premature anode-to-ignitor discharges. To keep the gallium in the liquid state, the base was kept at a constant 40 °C. This was first done using a cartridge heater embedded in the base and, when that failed unexpectedly, a flexible 100-W silicon tape heater was wrapped around the base of the glass tube.

The electrical schematic of the experimental setup in figure 5 shows a 10- $\mu$ F capacitor that is charged by a high-voltage power supply through a 50-k $\Omega$  charging resistor and discharged through the ignitron. The ignitor pulse was provided using a Perkin Elmer TM-11A high-voltage pulser capable of producing a 30-kV pulse with a pulse width of 4 ms. The discharge current was measured using a Pearson<sup>TM</sup> Electronics Model 1423 current monitor. The voltage across the capacitor was measured using a Tektronix P6015A 1,000:1 high-voltage probe. The current and voltage probe data were acquired using a Tektronix TDS-5000 digital oscilloscope. Trigger timing pulses were provided by a Berkeley Nucleonics Model 555 pulse delay generator, with the trigger pulse to the ignitor pulser box optically isolated from the rest of the test setup. High-speed imaging was performed using a Shimadzu HPV-2 high-speed camera capable of imaging at up to 1 million fps with a minimum gate time of 125 ns.

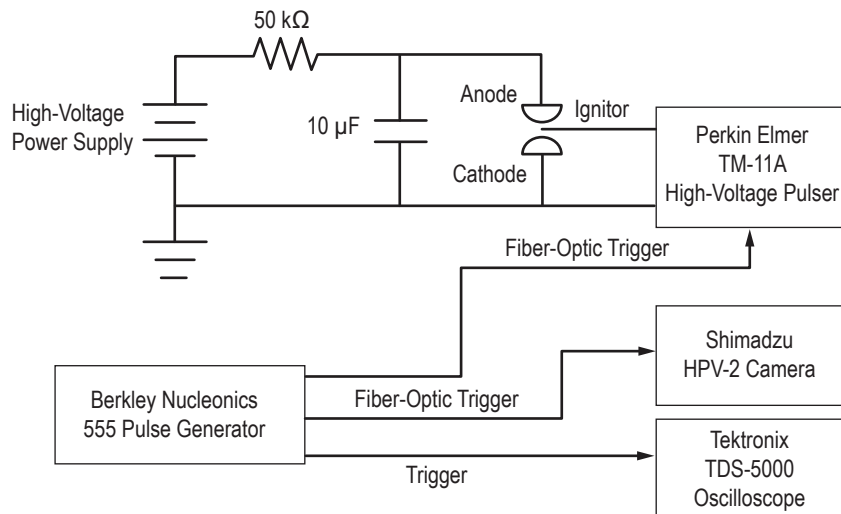


Figure 5. Schematic showing the setup of the ignitron charge circuit, trigger pulse paths, and data systems used.

## 5. EXPERIMENTAL DATA

Data are presented in this section for operation at charge voltages of 2 and 3 kV. In table 2 is a comparison of the time it takes for the current level to reach 10% of its maximum value, defined as the ignitron delay time, and the time it takes for the current level to increase from 10% to 90% of the maximum value, defined as the rise time. There was considerable difficulty with consistency and jitter in the triggering of the device. While the delay times given are real data obtained from individual 2- and 3-kV discharge pulses, they should be considered as representative values to illustrate the reduction in delay associated with the higher charge voltage. Presented in figure 6 are the voltage and current waveforms for a 2-kV discharge, with the time for each image in figure 7 indicated on the waveforms. The images were acquired at a frame rate of 500 kHz and an exposure gate time of 250 ns. Similar current and voltage waveform data and photographs are presented in figures 8 and 9, respectively, for a 3-kV discharge. For all data, time ( $t=0$ ) corresponds to the time when the Berkley Nucleonics trigger box issued the signal to discharge the Perkin Elmer pulser through the ignitor electrode.

Table 2. Ignition delay and current rise time for 2- and 3-kV discharges.

Discharge (kV)	Ignition Delay ( $\mu$ s)	Rise Time ( $\mu$ s)
2	106	10
3	64	10

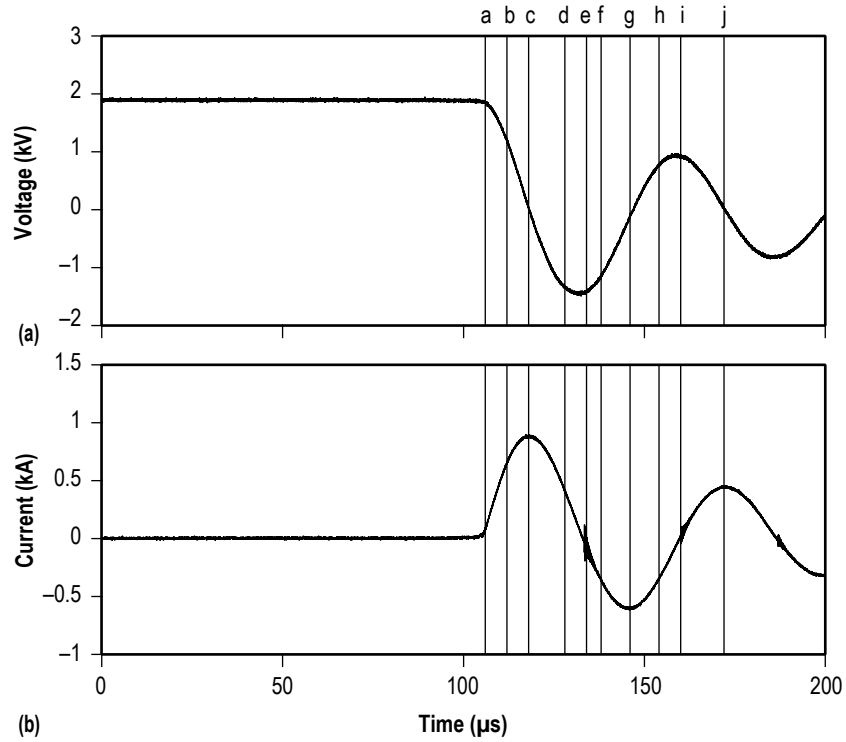


Figure 6. Waveforms for (a) voltage and (b) current for a 2-kV gallium ignitron discharge with markers indicating the times for the images in figure 7.

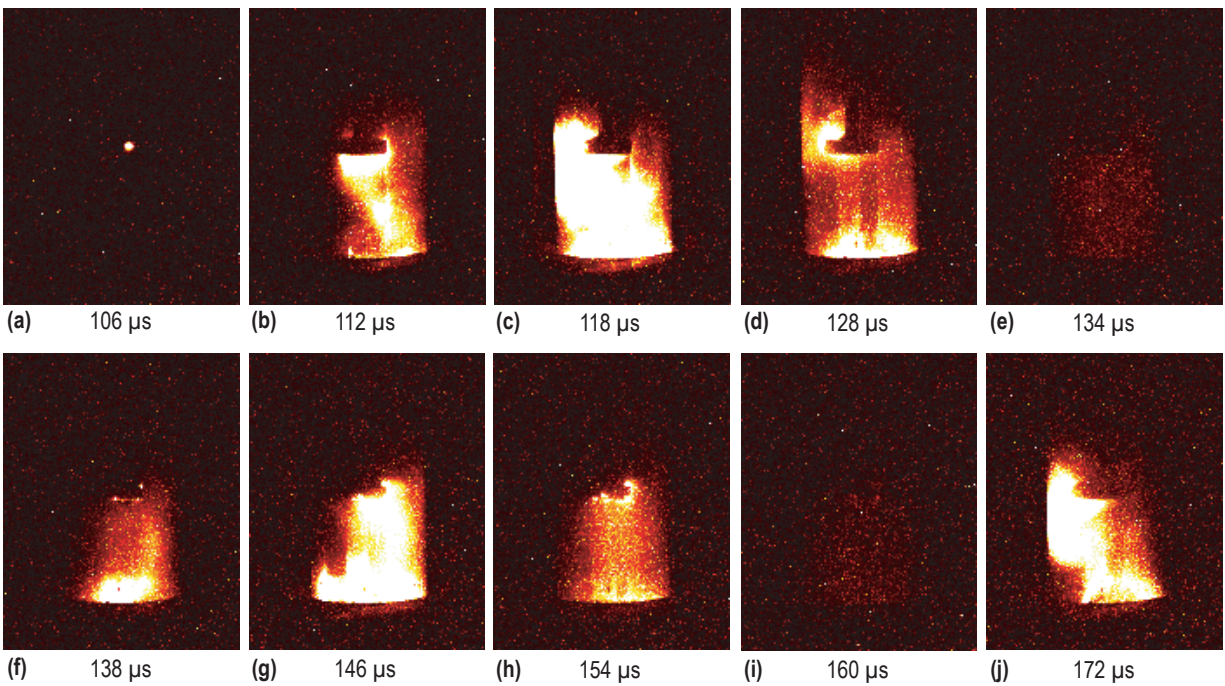


Figure 7. Selected images of a 2-kV gallium ignitron discharge obtained at a frame rate of 500 kHz and a gate time of 250 ns (false color of grayscale images). The subfigures correspond to the letters given on the waveforms in figure 6.



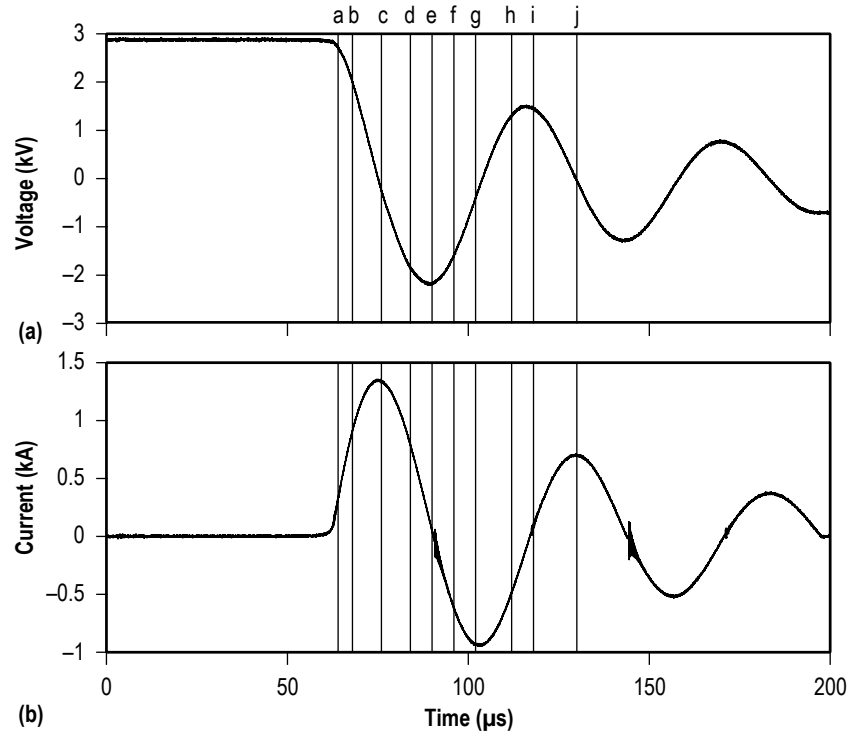


Figure 8. Waveforms for (a) voltage and (b) current for a 3-kV gallium ignitron discharge with markers indicating the times for the images in figure 9.

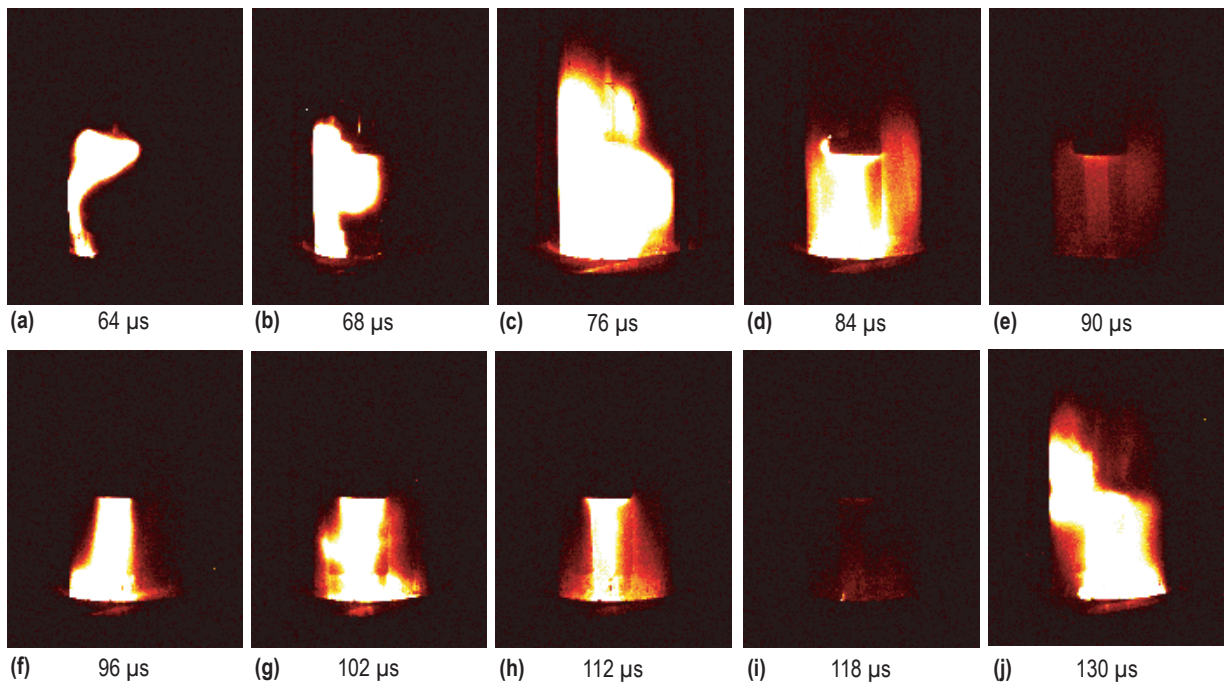


Figure 9. Selected images of a 3-kV gallium ignitron discharge obtained at a frame rate of 500 kHz and a gate time of 250 ns (false color of grayscale images). The subfigures correspond to the letters given on the waveforms in figure 8.

## 6. DISCUSSION

The frames in figures 7 and 9 show that the discharge light emission is much greater for the higher charge voltage, which is expected since the commensurate current levels are also significantly greater at the higher charge voltage. The higher energy in the 3-kV case leads to a much brighter discharge, and during the second half-cycle, the visible discharge appears very symmetric and well formed along the centerline. For both charge voltages, light emission during the first half-cycle begins at the anode and progresses to the cathode. In both figures 6 and 8, one observes little activity immediately after the trigger pulse at  $t=0$ , but once conduction occurs, peak current is reached with a rise time of 10  $\mu\text{s}$ . Since this is an underdamped, resistive-inductive-capacitive circuit, the discharge current oscillates as a damped sinusoid, completing several half-cycles of successively lower peak current levels before finally extinguishing when the bank voltage can no longer sustain the arc.

In figures 6 and 8, the time it takes for the current to reach 10% of peak current is much shorter for a higher applied voltage, occurring at  $t=106 \mu\text{s}$  and  $t=64 \mu\text{s}$  for the 2- and 3-kV cases, respectively. This delay is undesirable for ignitron operation because it can be a huge source of jitter in a pulsed system. As a point of comparison, the delay in a mercury-based ignitron would be on the order of 1  $\mu\text{s}$  or less.<sup>1</sup> In any ignitron, the delay between the initial trigger pulse and the time when current begins to flow scales with the time it takes for the plasma density to climb until a self-sustaining arc breakdown occurs at some critical density. The fact that at either charge voltage there is comparatively little variability in the time it takes to reach peak current once the discharge has been initiated indicates that the arc is self-sustaining once started, with the gallium ignition difficulty occurring due to the increased energy required to initially vaporize gallium as compared to mercury. This hypothesis is supported by the properties given in table 1, which show that gallium has a much higher heat of vaporization than mercury. An advantage gallium offers over mercury is a first ionization potential that is roughly half that of mercury, leading to the conclusion that maintaining a sufficient ionization fraction in the discharge once started is not a significant issue, as was seen in the self-sustaining nature of the discharge. It is noted that several ignition pulses failed to initiate conduction between the anode and cathode when provided an ignition pulse from the TM-11A. Only after being left at a vacuum level of  $10^{-5}$  torr or lower for an extended period of time would the ignitron fire reliably.

## 7. FUTURE DESIGN IMPROVEMENTS

In future design iterations, more effort should be placed on the fabrication of an ignitron that seals and holds internal vacuum conditions. While not quantitatively measured, it appeared that gallium oxide was forming on and wetting the various surfaces in the ignitron, including those fabricated from stainless steel and glass. This oxidation could be mitigated by cleaning gallium before it was loaded into the ignitron. The oxide layer on gallium in a solid state can be removed with a dilute sulfuric acid solution and subsequent washing with deionized water. This clean, solid gallium could then be loaded under an argon gas atmosphere to prevent reoxidation of the surface. The gallium can be melted and transferred to the glass vessel under such a neutral cover gas, with high-vacuum conditions in the ignitron preventing further oxidation, especially if the other surfaces also have their oxidation layers removed.

The ignitor tip should be machined from stainless steel to be a pointed cone, rather than the manually sharpened tip used in the present iteration. This should concentrate the ignition pulse to a much smaller area, increasing the localized heating and gallium vaporization rate. The ignitor tip should be moved as close as possible to the liquid gallium surface without the two touching and subsequently bridge the gap through wetting. A more energetic custom ignitor circuit could be fabricated to possess at least four times more energy per pulse than the roughly 18–24 J per pulse used for mercury ignitrons. This modification, in combination with the physical alterations to the ignitor electrode, should help vaporize more gallium per pulse relative to the present work, providing more reliable pulse ignition. These changes can also reduce ignition delays, providing the capability to operate the switch at a higher maximum repetition rate. In future testing, it is also recommended to monitor not only the current and voltage on the primary discharge circuit, but also the ignitor circuit to provide more insight into these ignitron startup issues and yield a more comprehensive and quantitative picture of the discharge delay and timing jitter.

It can be observed in figure 3 that increasing the initial concentration of gallium vapor may be achieved through increased heating of the liquid gallium pool, and this could help in reliable discharge initiation. To implement this, the base could be fabricated from ceramic or stainless steel to withstand higher temperatures. Below about 500 K, the vapor pressure of gallium increases exponentially with the temperature, yielding roughly an order of magnitude increase for every 10 K temperature increment.

## 8. CONCLUSIONS

A prototype gallium-based ignitron was designed, fabricated, and tested at charge voltages of 2 and 3 kV and internal gas pressures of  $\approx 10^{-5}$  torr. Current and voltage waveforms and high-speed imagery were presented for both charge voltages, with both exhibiting a large delay between the time the ignitor was pulsed and the time that the ignitron pulse began. This delay was shorter for the 3-kV discharge, owing to the increased initial electric field in the device that drives a faster cascade breakdown process. Once the pulse began, defined as the time when the current reaches 10% of peak current, both the 2- and 3-kV data showed similar current rise times, though the higher energy in the 3-kV case resulted in a much greater current and brighter discharge. These data, specifically the delays, suggest that the ignition trigger pulse is not vaporizing enough of the gallium cathode material to permit the discharge to rapidly initiate. Suggestions on how to improve the design and optimize the trigger pulse to make the operation more robust with shorter delays were also presented.

## REFERENCES

1. Schaefer, G.; Kristiansen, M.; and Guenther, A.H. (eds.): *Gas Discharge Closing Switches*, in *Advances in Pulsed Power Technology*, Vol. 2, Plenum Press, New York, NY, 570 pp., 1990.
2. Markusic, T.E.: “Current Sheet Canting in Pulsed Electromagnetic Accelerators,” Ph.D. Dissertation, Princeton University, Princeton, NJ, 215 pp., June 2002.
3. Polzin, K.A.; and Pearson, J.B.: “Reduced Plating Ignitron,” U.S. Patent 8710726, April 29, 2014.
4. Tooker, J.F.; Huynh P.; and Street R.W.: “Solid-State High-Voltage Crowbar Utilizing Series-Connected Thyristors,” Paper Presented at 17th IEEE International Pulsed Power Conference, Washington, D.C., June 29–July 2, 2009.
5. Geiger, F.; Busse, C.A.; and Loehrke, R.I.: “The Vapor Pressure of Indium, Silver, Gallium, Copper, Tin, and Gold Between 0.1 and 3.0 Bar,” *Int. J. Thermophys.* Vol. 8, No. 4, pp. 425–436, doi:10.1007/BF00567103, July 1987.
6. Huber, M.L.; Laesecke, A.; and Friend, D.G.: “Correlation for the Vapor Pressure of Mercury,” *Ind. Eng. Chem. Res.*, Vol. 45, No. 21, doi:10.1021/ie060560s, pp. 7351–7361, September 2006.
7. Burke, J.E.: “Plasma Diagnostics on High Current Ignitrons,” Masters Thesis, Texas Tech University, Lubbock, TX, August 1989.

REPORT DOCUMENTATION PAGE			Form Approved OMB No. 0704-0188		
<p>The public reporting burden for this collection of information is estimated to average 1 hour per response, including the time for reviewing instructions, searching existing data sources, gathering and maintaining the data needed, and completing and reviewing the collection of information. Send comments regarding this burden estimate or any other aspect of this collection of information, including suggestions for reducing this burden, to Department of Defense, Washington Headquarters Services, Directorate for Information Operation and Reports (0704-0188), 1215 Jefferson Davis Highway, Suite 1204, Arlington, VA 22202-4302. Respondents should be aware that notwithstanding any other provision of law, no person shall be subject to any penalty for failing to comply with a collection of information if it does not display a currently valid OMB control number.</p> <p><b>PLEASE DO NOT RETURN YOUR FORM TO THE ABOVE ADDRESS.</b></p>					
1. REPORT DATE (DD-MM-YYYY) 01-02-2015		2. REPORT TYPE Technical Memorandum		3. DATES COVERED (From - To)	
4. TITLE AND SUBTITLE  Proof-of-Concept Experiments on a Gallium-Based Ignitron for Pulsed Power Applications			5a. CONTRACT NUMBER		
			5b. GRANT NUMBER		
			5c. PROGRAM ELEMENT NUMBER		
6. AUTHOR(S)  H.K. Ali, V.S. Hanson, K.A. Polzin, and J.B. Pearson			5d. PROJECT NUMBER		
			5e. TASK NUMBER		
			5f. WORK UNIT NUMBER		
7. PERFORMING ORGANIZATION NAME(S) AND ADDRESS(ES) George C. Marshall Space Flight Center Huntsville, AL 35812			8. PERFORMING ORGANIZATION REPORT NUMBER  M-1391		
9. SPONSORING/MONITORING AGENCY NAME(S) AND ADDRESS(ES) National Aeronautics and Space Administration Washington, DC 20546-0001			10. SPONSORING/MONITOR'S ACRONYM(S) NASA		
			11. SPONSORING/MONITORING REPORT NUMBER NASA/TM-2015-218202		
12. DISTRIBUTION/AVAILABILITY STATEMENT Unclassified-Unlimited Subject Category 33 Availability: NASA STI Information Desk (757-864-9658)					
13. SUPPLEMENTARY NOTES  Prepared by the Propulsion Systems Department, Engineering Directorate					
14. ABSTRACT Results of testing a gallium-based ignitron at charge voltages of 2 and 3 kV are presented. In this work, gallium is employed as an alternative to mercury, which is typically used in an ignitron but presents hazards and potential environmental issues. Data showing the discharge current and voltage are presented, with corresponding high-speed imagery providing additional insight into how the gallium ignitron is functioning. In both cases, there is a long delay between the issuing of the ignition pulse and the time when the majority of the discharge current begins to flow, though this delay is far shorter for the higher voltage case. The discharges both proceed in a similar fashion once the primary discharge current begins to flow, implying that the primary cause of the delay owes to an underpowered ignition pulse that is not vaporizing enough gallium to permit a fast breakdown in the device. Ideas based upon previous ignitron research are presented on how to improve the design to improve and optimize operation.					
15. SUBJECT TERMS ignitron, pulsed power, plasma switch, gallium, mercury					
16. SECURITY CLASSIFICATION OF:			17. LIMITATION OF ABSTRACT	18. NUMBER OF PAGES	19a. NAME OF RESPONSIBLE PERSON
a. REPORT	b. ABSTRACT	c. THIS PAGE			STI Help Desk at email: help@sti.nasa.gov
U	U	U	UU	32	19b. TELEPHONE NUMBER (Include area code) STI Help Desk at: 757-864-9658



National Aeronautics and  
Space Administration  
IS20  
**George C. Marshall Space Flight Center**  
Huntsville, Alabama 35812